ISSN 1512-1461

UDC: 538.9 Condensed matter Physics, Solid state Physics, Theoretical Condensed matter Physics

THIRD ORDER PERTURBED HEISENBERG HAMILTONIAN OF Fe_3O_4 ULTRA THIN FILMS

P. Samarasekara

Department of Physics, University of Peradeniya, Peradeniya, Sri Lanka

Abstract:
Ultra thin Fe_3O_4 films with 2 and 3 spin layers were described using third order perturbed Heisenberg Hamiltonian. 3- D graphs of energy versus angle and stress induced anisotropy were plotted for two and three spin layers in order to find the values of stress induced anisotropy corresponding to energy minima. Both graphs have energy minima at the same values of stress induced anisotropy. However, 3-D plots were slightly different in two cases. Using the values of stress induced anisotropy corresponding to energy minima, magnetic easy directions were found for films with two and three spin layers. Curves of magnetic energy versus angle were plotted to find magnetic easy and hard directions. Although a sin curve could be obtained for the film with two layers, a curve with some sharp maxima appear in the graph of film plotted for three layers. All the graphs were plotted using MATLAB software.

Keywords: *Third order perturbation, Hamiltonian, spin layers, Fe_3O_4 thin films*

1. Introduction:

Fe_3O_4 finds potential applications in magnetic storage, industrial catalysts, water purification and drug delivery. Fe_3O_4 is a ferrite with inverse spinel structure. Magnetite (Fe_3O_4) and maghemite (γFe_2O_3) are the most popular natural oxides. Spinel structure with tetrahedral and octahedral sites can be found in detail in some previous publications [1, 2, 3, 4, 5]. Five of Fe^{3+} ions occupy tetrahedral sites. Other five Fe^{3+} ions and four Fe^{2+} ions occupy octahedral sites. Because magnetic moments of Fe^{3+} in tetrahedral and octahedral sites cancel each other, the net magnetic moment of Fe_3O_4 is completely due to the magnetic moments of four Fe^{2+} ions. Therefore, the theoretical net magnetic moment of Fe_3O_4 is 4 Bohr magnetons. However, experimental value of net magnetic moment is approximately 4.1 Bohr magnetons. The spinel structure of this ferrite is represented by $Fe^{3+}(Fe^{2+}Fe^{3+})O_4$. The magnetic moments of Fe^{2+} and Fe^{3+} are 4 μ_B and 5 μ_B, respectively.

Surface spin waves in CsCl type ferrimagnet with a (001) surface has been studied by combining Green function theory with the transfer matrix method [6]. Cation distribution of ferrite like compounds has been found using Rietveld method [1, 2]. Anisotropy of ultrathin ferromagnetic films and the spin reorientation transition have been investigated using Heisenberg Hamiltonian with few terms [7]. In addition, the surface magnetism of ferrimagnet thin films has been studied using Heisenberg method [8]. The surface spin wave spectra of both the simple cubic and body centered ferrimagnets have been theoretically studied using Heisenberg Hamiltonian [9]. The cation distribution and oxidation state of Mn-Fe spinel nanoparticles have been systematically studied at various temperatures by using neutron diffraction and electron energy loss spectroscopy [4]. The crystal structure of spinel type compounds has been found using single crystal X-ray diffraction data [3]. The lattice parameter, anion parameter and the cation inversion parameter of spinel structures have been presented [5]. Surface spin waves on the (001) free surface of semi-infinite two lattice ferrimagnets on the Heisenberg model with nearest neighbor exchange interactions has been investigated [10].

Ferromagnetic ultra-thin and thick films have been investigated using second order perturbed Heisenberg Hamiltonian by us [11]. Previously ferromagnetic ultra thin and thick films have been studied using third order perturbed Heisenberg Hamiltonian [12, 13]. Furthermore, ferrite ultra-thin

ISSN 1512-1461

and thick films have been investigated using second order perturbed Heisenberg Hamiltonian by us [14, 15]. Ferrite ultra-thin and thick films have been investigated using third order perturbed Heisenberg Hamiltonian [16, 17]. In this manuscript, the third order perturbed Heisenberg Hamiltonian was used to describe Fe_3O_4 ultra thin films.

2. Model:

Classical Heisenberg Hamiltonian of a thin film can be written as following.

$$H= -J\sum_{m,n}\vec{S}_m.\vec{S}_n + \omega\sum_{m\neq n}\left(\frac{\vec{S}_m.\vec{S}_n}{r_{mn}^{3}} - \frac{3(\vec{S}_m.\vec{r}_{mn})(\vec{r}_{mn}.\vec{S}_n)}{r_{mn}^{5}}\right) - \sum_m D_{\lambda_m}^{(2)}(S_m^{z})^2 - \sum_m D_{\lambda_m}^{(4)}(S_m^{z})^4$$
$$-\sum_m \vec{H}..\vec{S}_m - \sum_m K_s Sin2\theta_m \qquad (1)$$

Here J, ω, θ, $D_m^{(2)}, D_m^{(4)}, H_{in}, H_{out}, K_s$, m, n and N are spin exchange interaction, strength of long range dipole interaction, azimuthal angle of spin, second and fourth order anisotropy constants, in plane and out of plane applied magnetic fields, stress induced anisotropy constant, spin plane indices and total number of layers in film, respectively. When the stress applies normal to the film plane, the angle between m^{th} spin and the stress is θ_m.

The cubic cell was divided into 8 spin layers with alternative A and Fe spins layers. The spins of A and Fe will be taken as 1 and p, respectively. While the spins in one layer point in one direction, spins in adjacent layers point in opposite directions. A thin film with (001) spinel cubic cell orientation will be considered. The length of one side of unit cell will be taken as “a”. Within the cell the spins orient in one direction due to the super exchange interaction between spins (or magnetic moments). Therefore the results proven for oriented case in one of our early report [14] will be used for following equations. But the angle θ will vary from θ_m to θ_{m+1} at the interface between two cells.

For a thin film with thickness Na,

Spin exchange interaction energy=$E_{exchange}$= $N(-10J+72Jp-22Jp^2)+8Jp\sum_{m=1}^{N-1}\cos(\theta_{m+1}-\theta_m)$

Dipole interaction energy=E_{dipole}

$$E_{dipole} = -48.415\omega\sum_{m=1}^{N}(1+3\cos 2\theta_m) + 20.41\omega p\sum_{m=1}^{N-1}[\cos(\theta_{m+1}-\theta_m)+3\cos(\theta_{m+1}+\theta_m)]$$

Here the first and second term in each above equation represent the variation of energy within the cell [14] and the interface of the cell, respectively. Then total energy is given by

$$E= N(-10J+72Jp-22Jp^2)+8Jp\sum_{m=1}^{N-1}\cos(\theta_{m+1}-\theta_m)$$
$$-48.415\omega\sum_{m=1}^{N}(1+3\cos 2\theta_m) + 20.41\omega p\sum_{m=1}^{N-1}[\cos(\theta_{m+1}-\theta_m)+3\cos(\theta_{m+1}+\theta_m)]$$
$$-\sum_{m=1}^{N}[D_m^{(2)}\cos^2\theta_m + D_m^{(4)}\cos^4\theta_m]$$
$$-4(1-p)\sum_{m=1}^{N}[H_{in}\sin\theta_m + H_{out}\cos\theta_m + K_s\sin 2\theta_m] \qquad (2)$$

Here the anisotropy energy term and the last term have been explained in our previous report for oriented spinel ferrite [14]. If the angle is given by $\theta_m=\theta+\varepsilon_m$ with perturbation ε_m, after taking the terms up to third order perturbation of ε,

The total energy can be given as $E(\theta)=E_0+E(\varepsilon)+E(\varepsilon^2)+E(\varepsilon^3)$

Here

ISSN 1512-1461

E_0= -10JN+72pNJ-22Jp^2N+8Jp(N-1)-48.415ωN-145.245ωNcos(2θ)
+20.41ωp[(N-1)+3(N-1)cos(2θ)]

$$-\cos^2\theta\sum_{m=1}^{N} D_m{}^{(2)} - \cos^4\theta\sum_{m=1}^{N} D_m{}^{(4)} - 4(1-p)N(H_{in}\sin\theta + H_{out}\cos\theta + K_s\sin 2\theta) \qquad (3)$$

$$E(\varepsilon) = 290.5\omega\sin(2\theta)\sum_{m=1}^{N}\varepsilon_m - 61.23\omega p\sin(2\theta)\sum_{m=1}^{N-1}(\varepsilon_m + \varepsilon_n)$$
$$+\sin 2\theta\sum_{m=1}^{N} D_m{}^{(2)}\varepsilon_m + 2\cos^2\theta\sin 2\theta\sum_{m=1}^{N} D_m{}^{(4)}\varepsilon_m$$
$$+4(1-p)[-H_{in}\cos\theta\sum_{m=1}^{N}\varepsilon_m + H_{out}\sin\theta\sum_{m=1}^{N}\varepsilon_m - 2K_s\cos 2\theta\sum_{m=1}^{N}\varepsilon_m] \qquad (4)$$

$$E(\varepsilon^2) = -4Jp\sum_{m=1}^{N-1}(\varepsilon_n - \varepsilon_m)^2 + 290.5\omega\cos(2\theta)\sum_{m=1}^{N}\varepsilon_m{}^2 - 10.2\omega p\sum_{m=1}^{N-1}(\varepsilon_n - \varepsilon_m)^2$$
$$-30.6\omega p\cos(2\theta)\sum_{m=1}^{N-1}(\varepsilon_n + \varepsilon_m)^2$$
$$-(\sin^2\theta - \cos^2\theta)\sum_{m=1}^{N} D_m{}^{(2)}\varepsilon_m{}^2 + 2\cos^2\theta(\cos^2\theta - 3\sin^2\theta)\sum_{m=1}^{N} D_m{}^{(4)}\varepsilon_m{}^2$$
$$+4(1-p)[\frac{H_{in}}{2}\sin\theta\sum_{m=1}^{N}\varepsilon_m{}^2 + \frac{H_{out}}{2}\cos\theta\sum_{m=1}^{N}\varepsilon_m{}^2 + 2K_s\sin 2\theta\sum_{m=1}^{N}\varepsilon_m{}^2] \qquad (5)$$

$$E(\varepsilon^3) = 10.2p\omega\sin 2\theta\sum_{m,n=1}^{N}(\varepsilon_m + \varepsilon_n)^3 - 193.66\omega\sin 2\theta\sum_{m=1}^{N}\varepsilon_m{}^3 - \frac{4}{3}\cos\theta\sin\theta\sum_{m=1}^{N} D_m{}^{(2)}\varepsilon_m{}^3$$
$$-4\cos\theta\sin\theta(\frac{5}{3}\cos^2\theta - \sin^2\theta)\sum_{m=1}^{N} D_m{}^{(4)}\varepsilon_m{}^3$$
$$+4(1-p)[\frac{H_{in}}{6}\cos\theta\sum_{m=1}^{N}\varepsilon_m{}^3 - \frac{H_{out}}{6}\sin\theta\sum_{m=1}^{N}\varepsilon_m{}^3 + \frac{4K_s}{3}\cos 2\theta\sum_{m=1}^{N}\varepsilon_m{}^3]$$

The sin and cosine terms in equation number 2 have been expanded to obtain above equations. Here n=m+1.

Under the constraint $\sum_{m=1}^{N}\varepsilon_m = 0$, first and last three terms of equation 4 are zero.

Therefore, E(ε)=$\vec{\alpha}.\vec{\varepsilon}$

Here $\vec{\alpha}(\varepsilon) = \vec{B}(\theta)\sin 2\theta$ are the terms of matrices with

$$B_\lambda(\theta) = -122.46\omega p + D_\lambda{}^{(2)} + 2D_\lambda{}^{(4)}\cos^2\theta \qquad (6)$$

Also $E(\varepsilon^2) = \frac{1}{2}\vec{\varepsilon}.C.\vec{\varepsilon}$, and matrix C is assumed to be symmetric (C_{mn}=C_{nm}).

Here the elements of matrix C can be given as following,

$C_{m,\,m+1}$=8Jp+20.4ωp-61.2pωcos(2θ)

For m=1 and N,

C_{mm}= -8Jp-20.4ωp-61.2pωcos(2θ)+581ωcos(2θ) $-2(\sin^2\theta - \cos^2\theta)\ D_m{}^{(2)}$

$$+4\cos^2\theta(\cos^2\theta - 3\sin^2\theta)\ D_m{}^{(4)} + 4(1-p)[H_{in}\sin\theta + H_{out}\cos\theta + 4K_s\sin(2\theta)] \qquad (7)$$

For m=2, 3, ----, N-1

C_{mm}= -16Jp-40.8ωp-122.4pωcos(2θ)+581ωcos(2θ) $-2(\sin^2\theta - \cos^2\theta)\ D_m{}^{(2)}$

$$+4\cos^2\theta(\cos^2\theta - 3\sin^2\theta)\ D_m{}^{(4)} + 4(1-p)[H_{in}\sin\theta + H_{out}\cos\theta + 4K_s\sin(2\theta)]$$

ISSN 1512-1461

Otherwise, $C_{mn}=0$

Also $E(\varepsilon^3)=\varepsilon^2\beta.\vec{\varepsilon}$

Here matrix elements of matrix β can be given as following.

When m=1 and N,

$$\beta_{mm}=-193.66\omega\sin2\theta+10.2p\omega\sin2\theta-\frac{4}{3}\cos\theta\sin\theta D_m^{(2)}$$
$$-4\cos\theta\sin\theta(\frac{5}{3}\cos^2\theta-\sin^2\theta)D_m^{(4)}+4(1-p)[\frac{H_{in}}{6}\cos\theta-\frac{H_{out}}{6}\sin\theta+\frac{4K_s}{3}\cos2\theta]$$

When m=2, 3, ------, N-1

$$\beta_{mm}=-193.66\omega\sin2\theta+20.4p\omega\sin2\theta-\frac{4}{3}\cos\theta\sin\theta D_m^{(2)}$$
$$-4\cos\theta\sin\theta(\frac{5}{3}\cos^2\theta-\sin^2\theta)D_m^{(4)}+4(1-p)[\frac{H_{in}}{6}\cos\theta-\frac{H_{out}}{6}\sin\theta+\frac{4K_s}{3}\cos2\theta]$$

$$\beta_{m,m+1}=30.6p\omega\sin2\theta \tag{8}$$

Otherwise $\beta_{nm}=0$. Also $\beta_{nm}=\beta_{mn}$ and matrix β is symmetric.

Therefore, the total magnetic energy given in equation 2 can be deduced to

$$E(\theta)=E_0+\vec{\alpha}.\vec{\varepsilon}+\frac{1}{2}\vec{\varepsilon}.C.\vec{\varepsilon}+\varepsilon^2\beta.\vec{\varepsilon} \tag{9}$$

Because the derivation of a final equation for ε with the third order of ε in above equation is tedious, only the second order of ε will be considered for following derivation.

Then $E(\theta)=E_0+\vec{\alpha}.\vec{\varepsilon}+\frac{1}{2}\vec{\varepsilon}.C.\vec{\varepsilon}$

Using a suitable constraint in above equation [13], it is possible to show that $\vec{\varepsilon}=-C^+.\vec{\alpha}$

Here C^+ is the pseudo-inverse given by

$$C.C^+=1-\frac{E}{N}. \tag{10}$$

E is the matrix with all elements given by $E_{mn}=1$.

After using ε in equation 9, $E(\theta)=E_0-\frac{1}{2}\vec{\alpha}.C^+.\vec{\alpha}$ - $(C^+\alpha)^2\vec{\beta}(C^+\alpha)$ (11)

3. Results and discussion:

The energy given in above equation 11 will be calculated for film with two layers (N=2). The equations will be proven under the assumption of $D_1^{(2)}=D_2^{(2)}$ and $D_1^{(4)}=D_2^{(4)}$. According to above equations, $C_{11}=C_{22}$ and $C_{12}=C_{21}$.

Therefore from equation 10, $C^+{}_{12}=C^+{}_{21}=\dfrac{1}{2(C_{21}-C_{22})}=-C^+{}_{11}=-C^+{}_{22}$

Using above results, $\vec{\alpha}.C^+.\vec{\alpha}=(\alpha_1-\alpha_2)^2C^+{}_{11}$

But from equation 6, for a film with two layers $\alpha_1=\alpha_2$. Therefore, $\vec{\alpha}.C^+.\vec{\alpha}=0$.

Also $(C^+\alpha)^2\vec{\beta}(C^+\alpha)=(C_{11}^+\alpha_1+C_{12}^+\alpha_2)^2[\beta_{11}(C_{11}^+\alpha_1+C_{12}^+\alpha_2)$
$+\beta_{12}(C_{21}^+\alpha_1+C_{22}^+\alpha_2)]$
$+(C_{21}^+\alpha_1+C_{22}^+\alpha_2)^2[\beta_{21}(C_{11}^+\alpha_1+C_{12}^+\alpha_2)$
$+\beta_{22}(C_{21}^+\alpha_1+C_{22}^+\alpha_2)]$ (12)

ISSN 1512-1461

If $C^{+}{}_{12} = -C^{+}{}_{11}$ and $C^{+}{}_{21} = -C^{+}{}_{22}$, and $\alpha_1=\alpha_2$, then $(C^{+}\alpha)^2 \vec{\beta}(C^{+}\alpha)=0$.
When anisotropy constant varies within the film, $C_{12}=C_{21}$ and $C_{22} \neq C_{11}$.

Therefore, $C^{+}{}_{11} = -C^{+}{}_{12} = \dfrac{C_{22}+C_{21}}{2(C_{11}C_{22}-C_{21}{}^2)}$ and $C^{+}{}_{21} = -C^{+}{}_{22} = \dfrac{C_{21}+C_{11}}{2(C_{21}{}^2-C_{11}C_{22})}$.

Hence, $\vec{\alpha}.C^{+}.\vec{\alpha} = (\alpha_1-\alpha_2)\ (C^{+}{}_{21}\alpha_2 - C^{+}{}_{12}\alpha_1)$

If all the terms are considered, the $C_{11}C_{22}$ product will consist of 80 terms. Therefore, only the magnetic exchange energy, second order anisotropy, and the stress induced anisotropy terms will be considered for this simulation.
For Fe_3O_4, p=5/4=1.25.

C_{11}= -10J-25.5ω+504.5ωcos(2θ) $+ 2(\cos 2\theta)\ D_1^{(2)}$ -4$K_s$sin(2θ)

C_{22}= -10J-25.5ω+504.5ωcos(2θ) $+ 2(\cos 2\theta)\ D_2^{(2)}$ -4$K_s$sin(2θ)

C_{12}=10J+25.5ω-76.5ωcos(2θ)

E_0= 101.25J-71.32ω-214ωcos(2θ) $-\cos^2\theta[D_1^{(2)}+D_2^{(2)}]$ +2$K_s$sin(2θ)

α_1=[-153.08ω+$D_1^{(2)}$]sin(2θ)

α_2=[-153.08ω+$D_2^{(2)}$]sin(2θ)

$$\beta_{11} = -180.91\omega\sin(2\theta) - 0.67\sin 2\theta D_1^{(2)} - \frac{4}{3}K_s\cos 2\theta$$

$$\beta_{22} = -180.91\omega\sin(2\theta) - 0.67\sin 2\theta D_2^{(2)} - \frac{4}{3}K_s\cos 2\theta$$

β_{12}=38.25ωsin2θ
Finally from equation 12,

$$(C^{+}\alpha)^2 \vec{\beta}(C^{+}\alpha) = (\alpha_1-\alpha_2)^3 \frac{\beta_{11}(C_{22}+C_{21})^3 + \beta_{22}(C_{21}+C_{11})^3}{8(C_{11}C_{22}-C_{21}{}^2)^3}$$

The total energy can be found from equation 11. Figure 1 shows the 3-D plot of $\frac{E(\theta)}{\omega}$ versus θ and $\frac{K_s}{\omega}$ for N=2. Other values were kept at $\frac{J}{\omega} = \frac{D_1^{(2)}}{\omega} = 10$ and $\frac{D_2^{(2)}}{\omega} = 5$. Energy minima could be observed at $\frac{K_s}{\omega}$=3, 5, 7, -----etc. Energy maxima could be observed at $\frac{K_s}{\omega}$=2, 5, 6, ----etc. Energy maxima and minima correspond to magnetic hard and easy directions. Magnetic easy directions can be observed at $\frac{K_s}{\omega}$=3, 5, 7, -----etc. This means that the film can be easily magnetized along some specific directions by applying a certain stress. The stress arises due to the difference between thermal expansion coefficients of film and the substrate during the cooling or heating process. Although this 3-D plot is similar to that of nickel ferrite ultra thin films obtained using the second order perturbed Heisenberg Hamiltonian, the energy of nickel ferrite film is much higher than that Fe_3O_4 films [14]. However, this 3-D plot is somewhat different from that of ultra thin ferromagnetic films found using third order perturbed Heisenberg Hamiltonian [13].

ISSN 1512-1461

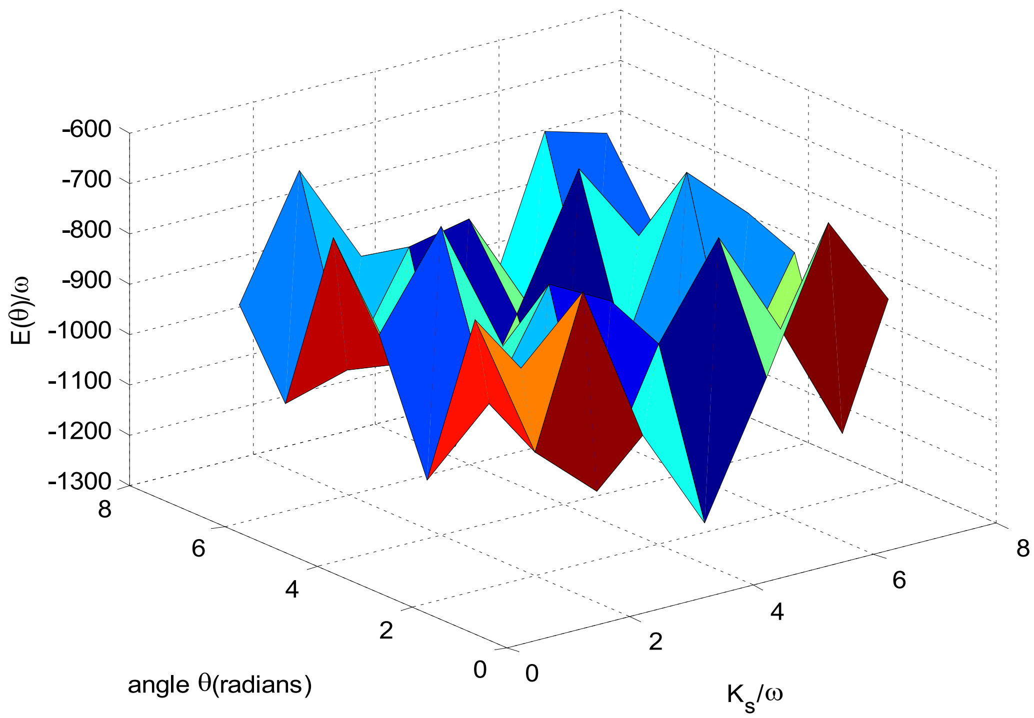

Figure 1: 3-D plot of $\frac{E(\theta)}{\omega}$ versus θ and $\frac{K_s}{\omega}$ for N=2.

Figure 2 shows the graph of energy versus angle for $\frac{K_s}{\omega}$=3. Energy minima can be observed at θ=3.1, 6.2 radians, ---- etc. Energy maxima can be observed at θ=1.5, 2.7, 7.8 radians, ----- etc. Magnetic easy directions are at θ=3.1, 6.2 radians, ---- etc. as measured with respect to the film normal. This curve is entirely different from that of thick ferromagnetic films obtained using third order perturbed Heisenberg Hamiltonian by us [12]. Similar to this curve, a smooth sin curve could be observed for thick ferromagnetic films obtained using third order perturbed Heisenberg Hamiltonian. According to our experimental data, the magnetic properties of nickel ferrite films depend on the stress induced anisotropy [18].

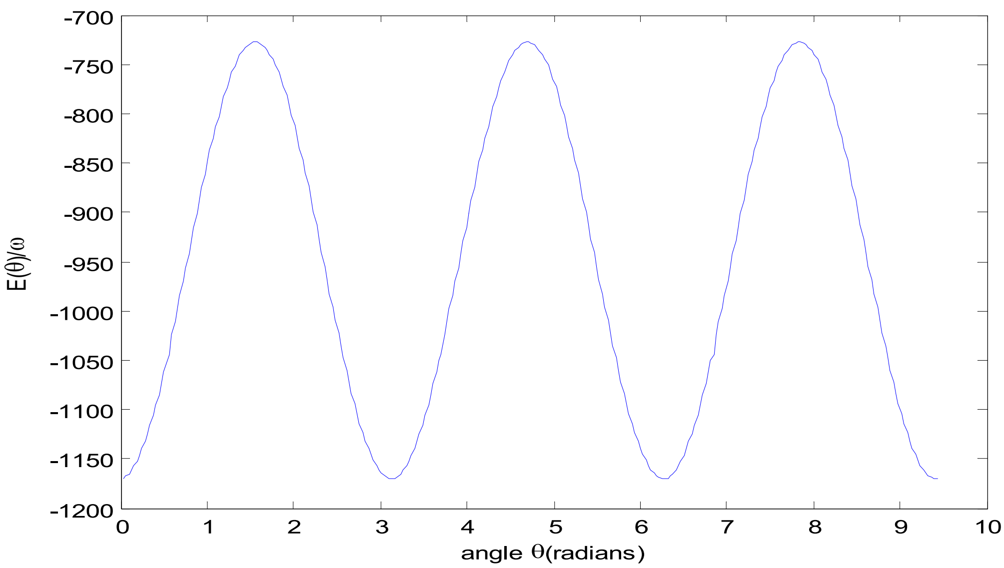

Figure 2: Graph of energy versus angle for $\frac{K_s}{\omega}$=3.

ISSN 1512-1461

When N=3, the each C^{+}_{nm} element found using equation 10 is consist of more than 20 terms. To avoid this problem, matrix elements were found using $C.C^{+}=1$. Then C^{+}_{mn} is given by $C^{+}_{mn} = \frac{cofactor C_{nm}}{\det C}$. Under this condition, $\vec{E}.\vec{\alpha} = 0$, and the average value of first order perturbation is zero. The second order anisotropy constant is assumed to be a constant within the film for the convenience.
Then

$C_{11}=C_{33}= -10J-25.5\omega+504.5\omega\cos(2\theta) + 2(\cos 2\theta)\, D_m^{(2)} -4K_s\sin(2\theta)$

$C_{22}= -20J-51\omega+428\omega\cos(2\theta) + 2(\cos 2\theta)\, D_m^{(2)} -4K_s\sin(2\theta)$

$C_{12}= C_{21}=C_{23}=C_{32}=10J+25.5\omega-76.5\omega\cos(2\theta)$

$C_{13}=C_{31}=0$

$\alpha=\alpha_1=\alpha_2=\alpha_3=(-153.08\omega + D_m^{(2)})\sin 2\theta$.

Therefore, $C^{+}_{11} = \frac{C_{11}C_{22} - C_{32}^{2}}{C_{11}^{2}C_{22} - 2C_{32}^{2}C_{11}} = C^{+}_{33}, C^{+}_{13} = \frac{C_{32}^{2}}{C_{11}^{2}C_{22} - 2C_{32}^{2}C_{11}} = C^{+}_{31}$

$C^{+}_{12} = \frac{-C_{32}C_{11}}{C_{11}^{2}C_{22} - 2C_{32}^{2}C_{11}} = C^{+}_{21} = C^{+}_{23} = C^{+}_{32}, C^{+}_{22} = \frac{C_{11}^{2}}{C_{11}^{2}C_{22} - 2C_{32}^{2}C_{11}}$

$\vec{\alpha}.C^{+}.\vec{\alpha} = \alpha^2[2C^{+}_{11}+4C^{+}_{32}+2C^{+}_{31}+C^{+}_{22}]$

$E_0= 156.875J-94.22\omega-282.66\omega\cos(2\theta) - 3D_m^{(2)}\cos^2\theta +3K_s\sin(2\theta)$

$$\beta_{11} = \beta_{33} = -180.91\omega\sin(2\theta) - 0.67\sin 2\theta D_m^{(2)} - \frac{4}{3}K_s\cos 2\theta$$

$$\beta_{22} = -168.16\omega\sin(2\theta) - 0.67\sin 2\theta D_m^{(2)} - \frac{4}{3}K_s\cos 2\theta$$

$\beta_{12}=38.25\omega\sin2\theta$

$$(C^{+}\alpha)^2\vec{\beta}(C^{+}\alpha) = \alpha^3\beta_{11}\{\frac{2(C_{22}-C_{32})^3 + (C_{11}-2C_{32})^3}{(C_{11}C_{22}-2C_{32}^{2})^3}\}$$

Figure 3 shows the 3-D plot of $\frac{E(\theta)}{\omega}$ versus θ and $\frac{K_s}{\omega}$ for N=3. Other values were kept at $\frac{J}{\omega} = \frac{D_m^{(2)}}{\omega} = 10$. Energy minima can be observed at $\frac{K_s}{\omega}$=3, 5, 7, ----- etc. Energy maxima can be observed at $\frac{K_s}{\omega}$=4, 6, ----- etc. Magnetic easy directions can be observed at $\frac{K_s}{\omega}$=3, 5, 7, ----- etc. Although the shape of this 3-D plot is slightly different from that of nickel ferrite ultra thin films obtained using third order perturbed Heisenberg Hamiltonian, both have almost the same maximum energy [16]. However, the shape of this 3-D plot is entirely different from that of nickel ferrite thick films obtained using third order perturbed Heisenberg Hamiltonian [17]. This graph is entirely different from the same graphs obtained for the thick nickel ferrite using the second order perturbed Heisenberg Hamiltonian [15]. In addition, the total energy of the thick film is 10^{11} time higher than that of ultra-thin film.

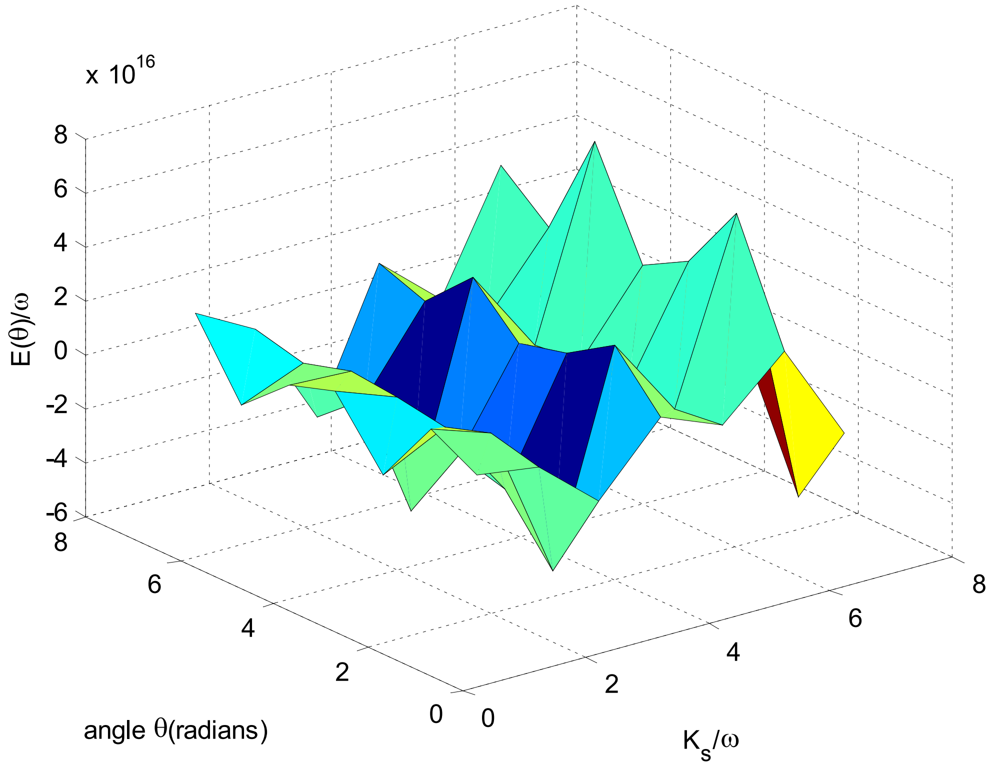

Figure 3: 3-D plot of $\frac{E(\theta)}{\omega}$ versus θ and $\frac{K_s}{\omega}$ for N=3.

Figure 4 shows the graph of $\frac{E(\theta)}{\omega}$ versus θ for $\frac{K_s}{\omega}$ =3. Energy minima can be observed at θ=0.75, 2.4, 3.9 radians, ----- etc. Energy maxima can be observed at θ=0.4, 3.5, 6.75 radians, ----- etc. Magnetic easy directions are θ=0.75, 2.4, 3.9 radians, ----- etc with respect to film normal. According to figures 2 and 4, the magnetic easy direction varies with the number of spin layers. The variation of magnetic easy direction with deposition temperature can be explained using Heisenberg Hamiltonian and idea of spin orientation [11, 19, 20].

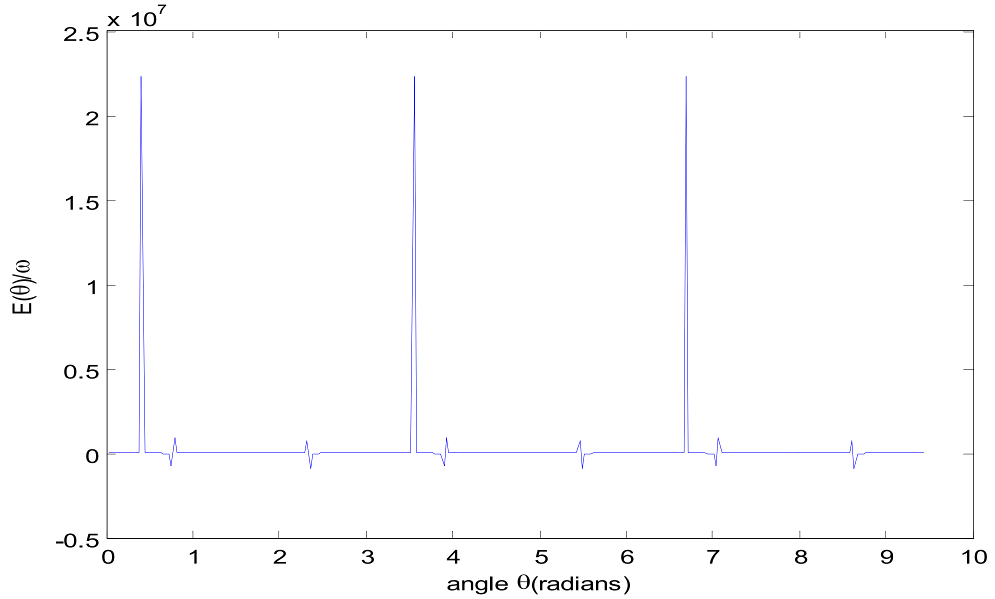

Figure 4: Graph of $\frac{E(\theta)}{\omega}$ versus θ for $\frac{K_s}{\omega}$ =3.

ISSN 1512-1461

4. Conclusion:

According to 3-D plots, Fe_3O_4 thin films with two and three spin layers can be easily magnetized along some directions under the influence of particular values of stress. For Fe_3O_4 films with two layers, energy becomes minimum at $\frac{K_s}{\omega}$ =3, 5, 7, -----etc. For $\frac{K_s}{\omega}$ =3 and N=2, magnetic easy directions were found to be θ=3.1, 6.2 radians, ---- etc. as measured with respect to the films normal. For Fe_3O_4 films with three layers, Energy minima can be observed at $\frac{K_s}{\omega}$ =3, 5, 7, ----- etc. For $\frac{K_s}{\omega}$ =3 and N=3, magnetic easy directions are θ=0.75, 2.4, 3.9 radians, ----- etc with respect to film normal. The shape of energy versus angle curve for N=2 is entirely different from that for N=3. However, the 3-D plot of N=2 is slightly different from that of N=3.

References:

1. I. S. Ahmed Farag, M. A. Ahmed, S.M. Hammad and A.M. Moustafa, Egyptian Journal of Solids (2001), 24(2), 215.
2. I. S. Ahmed Farag, M.A. Ahmed, S.M. Hammad and A.M. Moustafa, Crystal Research & Technology (2001), 36(1), 85.
3 V. Kahlenberg, C.S.J. Shaw and J.B. Parise, American Mineralogist (2001), 86, 1477.
4. Z. John Zhang, L. Zhong Wang, Bryan C. Chakoumakos and Jin S. Yin, Journal of the American Chemical Society (1998), 120(8), 1800.
5. E. Sickafus Kurt, John M. Wills and Norman W. Grimes, Journal of the American Ceramic Society (1999), 82(12), 3279.
6. S.T. Dai and Z.Y. Li, Physics Letters A (1990), 146, 450.
7. . K.D. Usadel and A. Hucht, Physical Review B (2002), 66, 024419.
8. Ding Ze-Nong, D.L. Lin and Libin Lin, Chinese Journal of Physics (1993), 31(3), 431.
9. D.H. Hung, I. Harada and O. Nagai, Physics Letters A (1975), 53(2), 157.
10. H. Zheng and D.L. Lin, Physical Review B (1988), 37(16), 9615.
11. P. Samarasekara and N.H.P.M. Gunawardhane, Georgian electronic scientific journals: Physics (2011), 2(6), 62.
12. P. Samarasekara, Electronic Journal of Theoretical Physics (2008), 5(17), 227.
13. P. Samarasekara and William A. Mendoza, Electronic Journal of Theoretical Physics (2010), 7(24), 197.
14. P. Samarasekara, M.K. Abeyratne and S. Dehipawalage, Electronic Journal of Theoretical Physics (2009), 6(20), 345.
15. P. Samarasekara, Georgian electronic scientific journals: Physics (2010), 1(3), 46.
16. P. Samarasekara and William A. Mendoza, Georgian Electronic Scientific Journals: Physics (2011), 1(5), 15.
17 P. Samarasekara, Inventi Rapid: Algorithm Journal (2011), 2(1), 1.
18. P. Samarasekara and F.J. Cadieu, Japanese Journal of Applied Physics (2001), 40, 3176.
19. P. Samarasekara and Udara Saparamadu, Georgian electronic scientific journals: Physics (2012), 1(7), 15.
20. P. Samarasekara and Udara Saparamadu, Research & Reviews: Journal of Physics-STM journals (2013), 2(2), 12.

Article received: 2020-01-29